Coral Reefs (2004) 23: 123–132
DOI 10.1007/s00338-003-0364-8

REPORT

Christopher D. Elvidge · John B. Dietz
Ray Berkelmans · Serge Andréfouët · William Skirving
Alan E. Strong · Benjamin T. Tuttle

Satellite observation of Keppel Islands (Great Barrier Reef) 2002 coral bleaching using IKONOS data

Received: 14 March 2003 / Accepted: 12 May 2003 / Published online: 7 February 2004

Abstract An examination of IKONOS satellite imagery of the Keppel Islands (Great Barrier Reef) acquired before and during a coral bleaching event indicates that severe bleaching of reefs can be detected as an increase in brightness in the band 1 (blue) and band 2 (green) IKONOS spectral bands (4-m resolution). The bleaching was not detected in band 3 (red), band 4 (near-infrared), or in the 1-m panchromatic band data. A total of 0.74 km^2 of bleached coral was identified, with detection occurring in waters as deep as 15 m. The procedure requires that one of the scenes be radiometrically normalized to match the reference scene prior to image differencing. A relative radiometric normalization was used in this case because variable cloud cover present in the image acquired during the bleaching event prevented reliable modeling of atmospheric effects. The success at coral bleaching detection at Keppel Islands represents both a "best-case" and a "cloud-challenged" scenario. It was a best-case scenario in that coral cover was extensive (70–90% live coral cover, mostly acroporids) and the bleaching level was extreme (92–95% of coral cover white bleached). It was a cloud-challenged scenario in terms of having extensive and highly variable cloud cover present in the image acquired during the bleaching event. Color difference images reveal extensive areas of bleached coral at sites away from our study area, indicating that this platform and methodology may be a valuable tool for mapping high coral cover areas during bleaching events. Additional studies and technique refinements would be required to test the detection limits of bleaching with IKONOS imagery or to develop a spectrally based bleaching detection index.

Keywords Coral bleaching · Remote sensing · Change detection

C. D. Elvidge (✉)
NOAA National Geophysical Data Center,
325 Broadway, Boulder, CO 80305, USA
E-mail: chris.elvidge@noaa.gov
Tel.: +1-303-4976121

J. B. Dietz
Cooperative Institute for Research in the Atmosphere,
Colorado State University, Fort Collins,
CO 80523, USA

R. Berkelmans
Australian Institute of Marine Science
and the CRC Reef Research Center,
4810 Townsville, Queensland,
Australia

S. Andréfouët
Institute for Marine Remote Sensing,
College of Marine Science,
University of South Florida,
St. Petersburg, FL 33701, USA

W. Skirving
Cooperative Institute for Research in the Atmosphere,
Colorado State University (NOAA-NESDIS
Office of Research and Applications),
Camp Springs, MD 20746, USA

A. E. Strong
NOAA NESDIS Office of Research and Applications,
Camp Springs, MD 20746, USA

B. T. Tuttle
Cooperative Institute for Research in Environmental Sciences,
University of Colorado, Boulder, CO 80305, USA

Present address: S. Andréfouët
UR Coreus—Institut de Recherche pour la
Développement (IRD), Nouvelle Calédonie

Introduction

During the past several decades, coral reefs in many parts of the world have been subjected to a series of bleaching events, including the Great Barrier Reef (GBR) in Australia (e.g. Berkelmans and Oliver 1999 and Berkelmans et al. this issue). Bleaching occurs when coral polyps expel the pigmented symbiotic algae, resulting in a bleached white appearance of living corals. Bleaching is believed to be induced when reef waters depart from the narrow range of environmental conditions (temperature, salinity, opacity, UV radiation, and nutrient levels) to which corals are adapted (Hoegh-Guldberg 1999). The rate and prospects for recovery of the coral from bleaching is highly variable. In some cases the polyps are able to recover their symbiotic algae (Hoegh-Guldberg 1999). However, severe or repeated bleaching can result in the death of polyps, which leaves the reef vulnerable to colonization by algae and structural collapse (Diaz-Pulido and McCook 2002).

Elevated water temperatures have been implicated in the majority of the large-scale coral bleaching events since the 1980s, and a number of SST indices have been developed to predict coral bleaching (e.g. Goreau and Hayes 1994; Podestá and Glynn 1997; Berkelmans et al. this issue). A recent experimental product from the National Oceanic and Atmospheric Administration (NOAA) is the satellite-derived Degree Heating Weeks (DHW) designed to indicate the accumulated thermal stress that coral reefs experience. The DHW index is formulated using a time series of satellite observations of sea surface temperature values. DHWs accumulate when the sea surface temperature is at least 1° C above the maximum expected summertime temperature. NOAA has correlated the DHW values to reports of bleaching and found that reefs subjected to DHWs of 8+ have been accompanied by severe bleaching and often mortality (Liu et al. 2003; Wellington et al. 2001).

Holden and LeDrew (1998) and Clark et al. (2000) acquired high-resolution reflectance spectra of coral and found that bleached coral is approximately 10% brighter in the visible spectrum than healthy coral, rising from about 10% reflectance to about 20%. Thus, bleached coral is approximately twice as bright as unbleached coral. However, these results do not consider the effects of the water column in preferentially absorbing longer wavelength light in the visible spectrum. Satellite detection of coral bleaching would require the penetration of sunlight through the water column, reflectance off the coral, and retransmission of the light up through the water column and the overlying atmosphere to a satellite sensor.

A wide range of phenomena affect the visibility of benthic features in satellite imagery, including the sensor characteristics, optical properties of the atmosphere (including clouds), the level of sunglint off the sea surface, and the inherent optical properties of the water column. Several studies have cast doubt on the prospects of detecting and quantifying coral bleaching from space. The detection of this brightening using satellite data is complicated by the small patch size of living corals on many reefs, spectral confusion with other bright benthic substrates (e.g. sand), and the attenuation of sunlight by the water and atmospheric columns. In addition, bleached coral may recover or become covered by algae within a few weeks or months of a bleaching event (Clark et al. 2000), reducing the temporal window within which bleaching could be detected. Recent studies conducted with Landsat Enhanced Thematic Mapper Plus data (Andréfouët et al. 2001) and Thematic Mapper data (Yamano and Tamura 2001) concluded that with 20- or 30-m spatial resolution data, the detection of coral bleaching would be probably restricted to areas with extensive stands of heavily bleached corals. Andréfouët et al. (2002) simulated 1-m resolution color imagery of reef areas from 10-cm aerial photography and concluded that even at this scale accurate quantification of coral bleaching requires heavy bleaching and extensive coral coverage.

Since late 1999 it has been possible to collect commercial satellite imagery in the 1–5 m range. The first such service to become available was IKONOS imagery, provided by Space Imaging. Panchromatic IKONOS data can be collected at 1-m spatial resolution. Four-band multispectral data can be collected at 4-m spatial resolution. The 11-bit radiometric resolution of IKONOS data offers increased discrimination of brightness levels above the 8-bit Landsat data, providing an additional sensitivity for demanding applications such as the detection of coral bleaching. In addition, the off-nadir pointing capabilities of the IKONOS sensor makes it possible to specify view angles that minimize image contamination from solar reflectance off the sea surface. Recent studies have confirmed that IKONOS data provide for enhanced mapping and monitoring capabilities for shallow water benthic communities when compared to Landsat and SPOT data (e.g. Mumby and Edwards 2002; Palandro et al. 2003; Capolsini et al. 2004).

This study is motivated by two objectives. The first objective is to test the feasibility of using high spatial resolution IKONOS imagery as a source of reference information on the presence or absence of bleached coral following the detection of SST anomalies. Because of the difficulty in acquiring timely field observations of coral bleaching the validation of SST-based predictors such as the DHW has been limited. If the occurrence and severity of bleaching could be confirmed using high spatial resolution satellite data, this information could be used to validate the bleaching alerts issued and lead to improvements in the alert thresholds. The second objective is to examine the potential value of IKONOS imagery as a source of information on the frequency, severity, and extent of coral bleaching for improved local-to-regional management and protection of reef resources. An IKONOS scene typically covers several hundreds of square kilometers, the size of many coral reef protected areas that require updated reef maps and assessments of perturbations such as coral bleaching to guide management decisions. For both objectives there is interest in testing the accuracy of qualitative bleaching detection (presence/absence) and quantitative data on the severity of bleaching (percent of bleached live coral cover).

Methods

Site selection

During late 2001 and early 2002, elevated in situ surface water temperatures (Berkelmans 2002) and associated coral bleaching (Fig. 1) were observed in several portions of the GBR. Simulta-

Fig. 1 Collection of underwater video data along a 50-m transect on February 27, 2002. Note the extensive cover of coral and the heavily bleached appearance. The tape marking the transect position can be seen running diagonally from the lower left corner

neously NOAA detected elevated sea surface temperatures with the DHW index and predicted coral bleaching. Based on the available information on where bleaching was occurring, a search was conducted of the IKONOS archive for imagery collected prior to the current bleaching event. Our strategy was to use a previously collected IKONOS image as a reference. The Great Keppel Island (GKI) area (Fig. 2) was chosen as our study area because of its high coral cover and the availability of ground-truth data.

Image acquisition/preprocessing

It was determined that the best archive scene of the GKI was taken August 22, 2001 (Fig. 3). This day provided both strikingly clear atmospheric and water conditions. Collection of new 1-m panchromatic and 4-m multispectral IKONOS imagery of the GKI was scheduled with Space Imaging in early April 2002. The collection constraints were that the sensor elevation had to be 70 to 85 degrees and viewing west from the east (view azimuth of 5 to 175 degrees). Images were acquired on April 15, 2002 and April 26, 2002. While neither image met the target of 80% cloud-free, the April 15 image had the lowest percentage of cloud cover (Fig. 3) and was selected for use in the study.

Data were processed with the dynamic range adjustment turned off. Space Imaging performed a standard radiometric correction as part of the product generation. The correction rescales the data from the satellite so that the same radiometric calibration coefficients can be applied to images acquired on different dates. Subsequent conversion from digital number (DN) to radiance L (in mW cm^{-2} sr^{-1}) follows the following format:

L = DN/calibration coefficient

Calibration coefficients are 633, 649, 840, and 746 mW cm^{-2} sr^{-1} for bands 1, 2, 3, and 4, respectively. Space Imaging provides no radiance calibration for the panchromatic band. The images were delivered in UTM projection, WGS-84 datum, via nearest-neighbor resampling. Table 1 provides the metadata of the two scenes.

Field observations

Underwater color video transects documenting reef conditions were acquired in four areas on February 25–27, 2002. The transects were acquired offshore from Middle and Halfway Islands (Fig. 2). At each island, a set of video transects was acquired from both slope and crest habitats of the reef (Fig. 1). Each set of transects consisted of five 50-m video swims. A GPS reading and direction bearing marked the location of the first transect. The positions of succeeding transects were placed on the satellite images based on a transect bearing and an offset from the previous transect. The video footages were each approximately 5 min in length and were analyzed according to standard video analysis procedures (Christi et al. 1996). This involved stopping the video 40 times along the length of each transect (evenly spaced stops). At each stop five points on the screen are assessed for the benthic cover (hard coral, soft coral, or other) and coral condition (white bleached, partially bleached, or not bleached) directly under each point. The 200 points are then used to calculate the percent cover of hard coral and soft coral and the percentage of coral in each of the above bleaching conditions.

Image coregistration

The April image was co-registered to the August image using image-to-image control points found near sea level on the islands present in the image pair. Control points included rocks, vegetation, and points selected at an airstrip. These points were selected by hand by an analyst viewing the two dates of imagery simultaneously. The April image was warped to fit over the August image using second order polynomial and nearest neighbor-resampling. For the multispectral image, 14 points were used, yielding a root mean square error of 0.532 pixels. The co-registration of the pan bands used nine points and yielded a root mean square error of 0.87 pixels. The co-registration of benthic features was examined visually by overlaying the August and warped April images and was found to be quite good. Factors which likely contributed to the ease and quality of the image co-registration include the similarity in the viewing geometry and tide stages (see Table 1).

Radiometric normalization

Before the August and April images could be quantitatively compared, the DN values in the two scenes had to be brought into accord. Because of the lack of field measurements, which could be used to convert the images to reflectance units and the widespread and variable thickness of cloud cover in the April image, a relative radiometric normalization was applied to the April data. The radiometric normalization was developed following the “pseudo-invariant feature” (PIF) methodology, described by Schott et al. (1988). This procedure makes use of bright and dark pixel sets extracted from the reference and subject images to define a gain and offset for normalizing the subject image to match the radiometry of the reference image.

As bright and dark features, we used white beach sand and submerged algal beds, respectively (Fig. 2). The DN pairs (April, August) for the PIF pixel sets were visually inspected on scattergrams (see Fig. 4) to check for anomalies. In each spectral band a small set of outlier pixels were found for the bright sand beach PIF pixel set. The outliers are undoubtedly due to minor variations in the surface reflectance of the beach sand between the two dates of

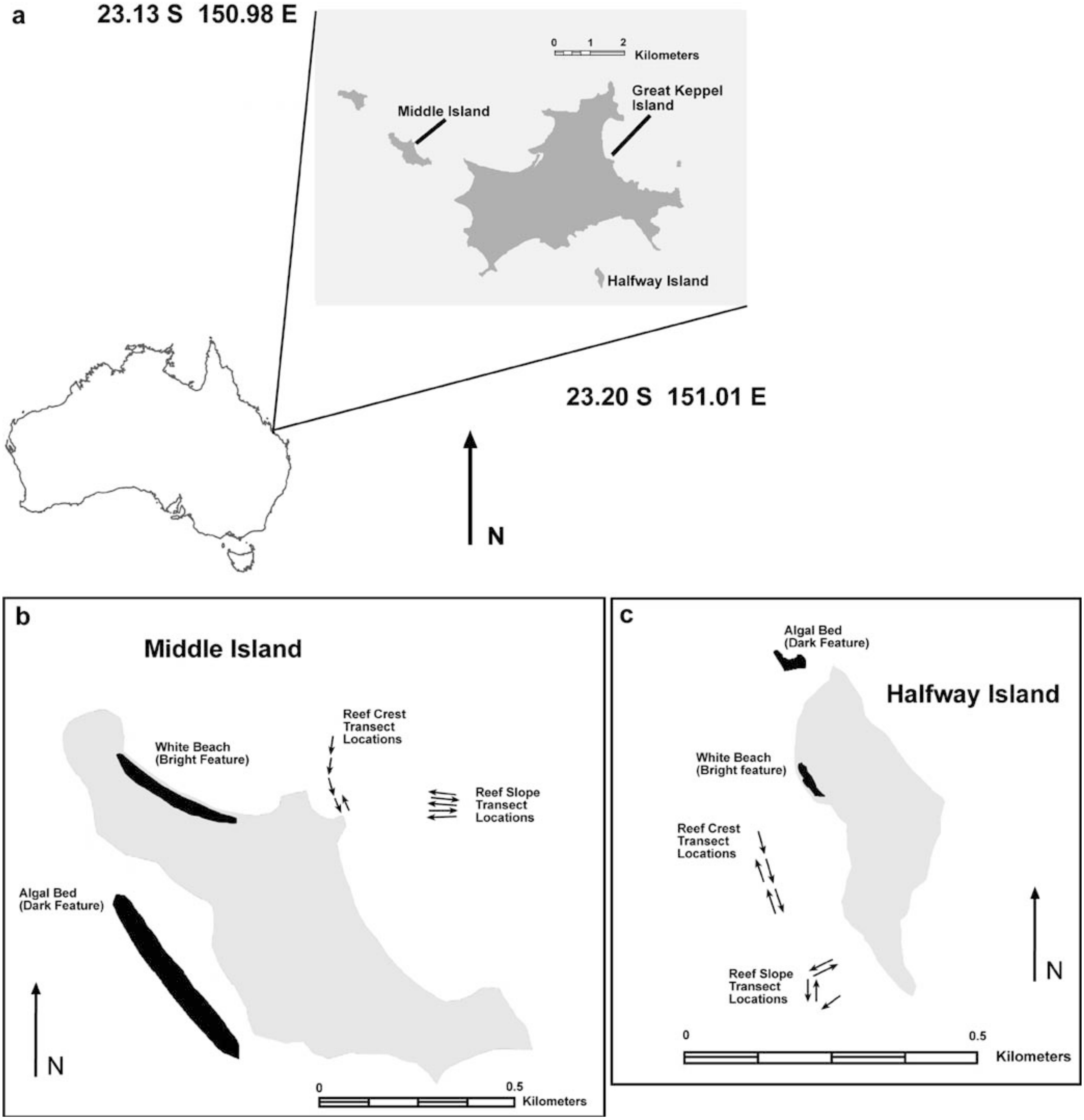

Fig. 2 **a** Location maps of the (**b**) Middle Island and (**c**) Halfway Island study areas, within the Keppel Islands, including locations of pseudo-invariant features used to intercalibrate the images

imagery. It may be that a handful of the selected pixels had wetter sand in one date relative to the other. While the cause of the outlier pixels may never be known, they were not excluded from the PIF analysis since they exerted a negligible effect on the outcome.

The light and dark PIF pixel sets were used as input into a linear regression statistical analysis, yielding a gain and offset used to convert the raw April DN into accord with the August DN, plus a regression coefficient (R^2 value) and a standard error (Table 2). The standard error has units of DN and provides an indication of the error or uncertainty of the relative radiometric normalization. Because of visible differences in the thickness of thin cloud cover between the Middle and Halfway Island study sites, a separate radiometric normalization was performed in each area. The radiometric normalization calculation was performed for each of the four multispectral bands and the panchromatic band. Then the gains and offsets were applied to the original April image data.

Extraction of spectral differences

Difference images were generated for each spectral band by subtracting the August 2001 digital numbers from the radiometrically normalized April 2002 digital numbers. Next, average DN spectra were extracted for the transect areas and two other benthic surfaces (white sand and silt). In addition average DN spectra were extracted from both dates of imagery for open water in an area covered by

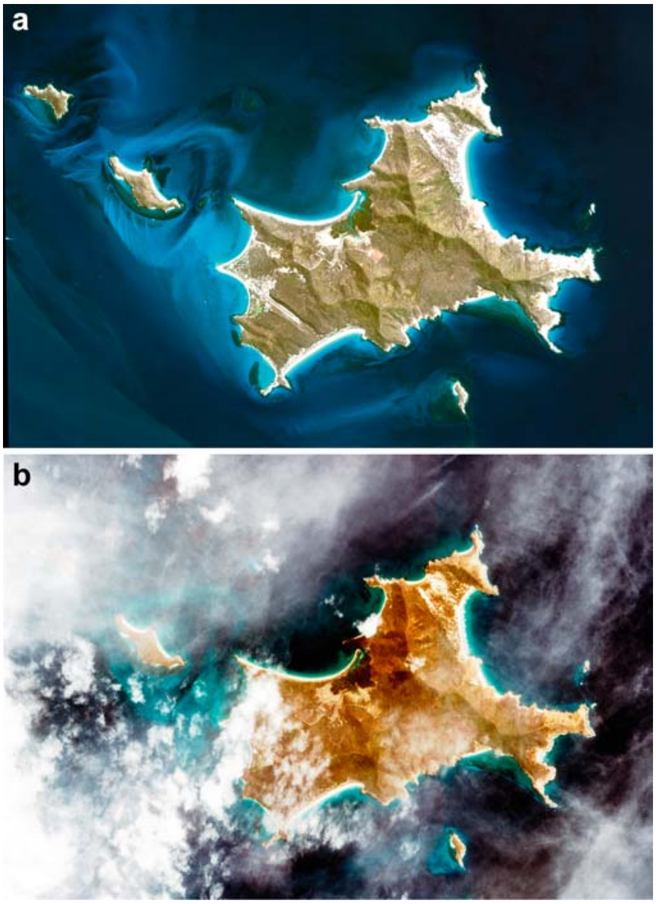

Fig. 3 August 22, 2001 (**a**) and April 15, 2002 (**b**) IKONOS images of the Keppel Islands. Bands 3, 2, 1 as RGB

Table 1 Metadata of the Great Keppel Island IKONOS images

Attribute	August 2001	April 2002
Acquisition date/GMT	2001-08-22/00:12	2002-04-15/00:15
Scene ID	2000010545902THC	2000013844800THC
Cloud cover	0%	More than 30%
Solar elevation angle	46.3	49.1
Solar azimuth angle	39.5	39.8
Sensor elevation angle	71.8	76.9
Collection azimuth angle	354.4	14.9
Tide height	3.04 m	3.55 m

clouds in the April image. For the multispectral bands the average DN spectra of the transect areas were converted to radiance units based on the coefficient factors supplied by Space Imaging.

Results

Field observations

Coral cover at both Middle and Halfway Islands was high, ranging from 73.1 to 95% (Table 3). Coral communities on the reef crest at both locations consisted predominantly of corymbose, plate, and staghorn *Acropora* sp. (Fig. 1), whereas on the reef slope, coral communities were almost exclusively made up of staghorn *Acropora* sp. Faviids, poritids, and pocilloporids made up less than 2% of the hard coral cover at all sites. Between 92 and 99% of the hard coral cover was bleached white, while only odd colonies retained some color or were visually well pigmented (Fig. 1, Table 3).

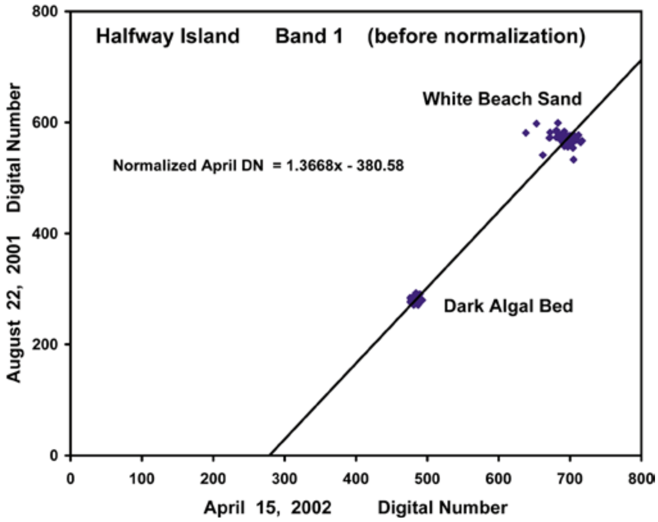

Fig. 4 Scattergram of the DN values for the dark algal bed and white beach sand pixel sets used as pseudo-invariant features for the Halfway Island study site. Overlaying the pixel data is the regression line

Table 2 Radiometric normalization regression results from Halfway Island. Gain and offset applied to the raw April DNs brings the values into accord with the August reference image

	Gain	Offset	R^2	Standard error
Band 1	1.367	−380.57	0.98	18.29
Band 2	1.420	−426.45	0.99	25.99
Band 3	1.565	−370.91	0.99	29.03
Band 4	1.648	−348.88	0.99	19.68
Panchromatic band	1.538	−355.90	0.99	20.19

Satellite observations

Table 4 presents the DN and radiance data extracted for the regions of interest coinciding with the transects, clouds present in the April image, and two additional benthic surface types (white sand and silt). When plotted as spectra (Fig. 5), it can be seen that the coral bleaching was detected as a brightening in band 1 and band 2. A t-test determined that the April band 1 and 2 data from the transect areas are significantly brighter than the pre-bleaching August data ($P < 0.0001$). The bleaching did not show up in band 3, band 4, or the panchromatic

Table 3 Percent cover of coral, white bleached coral, and partially bleached coral (± standard error, $n=5$ transects)

Middle Island		% Cover (± se)	% Cover of white bleached (± se)	% Cover of partial bleached (± se)
Crest	Hard coral	73.08 (8.06)	71.69 (8.23)	0.99 (0.38)
	Soft coral	3.92 (1.40)	1.69 (0.62)	0.20 (0.20)
Slope	Hard coral	73.98 (1.71)	73.44 (1.71)	0.25 (0.16)
	Soft coral	0.05 (0.38)	0	0
Halfway Island				
Crest	Hard coral	78.36 (4.59)	72.58 (4.41)	4.12 (0.59)
	Soft coral	0	0	0
Slope	Hard coral	94.99 (4.77)	90.29 (4.77)	4.51 (2.49)
	Soft coral	0.09 (0.09)	0	0

Table 4 Summary of IKONOS data from field transects

	August 22, 2001			April 15, 2002			April 15, 2002		
				Original			Normalized		
	Radiance in			Radiance in			Radiance in		
	DN Mean	mW Mean	$cm^{-2}sr^{-1}$ Std.Dev.	DN Mean	mW Mean	$cm^{-2}sr^{-1}$ Std.Dev.	DN Mean	mW Mean	$cm^{-2}sr^{-1}$ Std.Dev.
Halfway Island slope transects									
Band 1	273	0.375	0.003	538	0.730	0.01	355	0.488	0.015
Band 2	206	0.283	0.005	509	0.701	0.011	296	0.408	0.016
Band 3	82	0.086	0.002	291	0.307	0.004	86	0.091	0.006
Band 4	48	0.057	0.002	235	0.279	0.004	39	0.047	0.007
Pan band	95			312			128		
Halfway Island crest transects									
Band 1	277	0.381	0.004	526	0.723	0.006	339	0.466	0.009
Band 2	213	0.293	0.004	499	0.686	0.006	281	0.387	0.009
Band 3	83	0.088	0.002	287	0.303	0.003	80	0.084	0.004
Band 4	49	0.058	0.001	232	0.275	0.003	34	0.041	0.006
Pan band	98			306			118		
Middle Island slope transects									
Band 1	272	0.374	0.003	586	0.805	0.009	365	0.502	0.018
Band 2	204	0.281	0.004	577	0.794	0.011	313	0.43	0.023
Band 3	79	0.083	0.001	383	0.403	0.003	121	0.128	0.008
Band 4	46	0.054	0.001	316	0.375	0.004	75	0.089	0.009
Pan band	96			387			135		
Middle Island crest transects									
Band 1	275	0.379	0.004	605	0.831	0.012	403	0.554	0.024
Band 2	211	0.29	0.005	603	0.829	0.015	367	0.505	0.031
Band 3	82	0.086	0.003	408	0.430	0.011	179	0.188	0.027
Band 4	49	0.058	0.003	340	0.403	0.013	133	0.158	0.033
Pan band	104			406			175		
Benthic white sand									
Band 1	298	0.41	0.006	491	0.675	0.006	272	0.400	0.009
Band 2	218	0.30	0.007	455	0.626	0.007	200	0.303	0.011
Band 3	82	0.086	0.001	288	0.304	0.003	60	0.083	0.005
Band 4	50	0.059	0.002	240	0.285	0.004	25	0.054	0.006
Pan band	101			300			104		
Benthic silt									
Band 1	276	0.379	0.003	488	0.670	0.006	286	0.393	0.008
Band 2	194	0.267	0.002	449	0.617	0.007	211	0.290	0.010
Band 3	79	0.083	0.001	296	0.312	0.005	91	0.096	0.008
Band 4	45	0.054	0.002	236	0.280	0.005	39	0.046	0.008
Pan band	105			299			103		
Clouds									
Band 1	287	0.394	0.003	660	0.906	0.063	521	0.715	0.087
Band 2	206	0.283	0.003	663	0.913	0.081	516	0.710	0.115
Band 3	79	0.083	0.002	486	0.512	0.056	387	0.408	0.088
Band 4	45	0.054	0.001	403	0.478	0.055	312	0.370	0.090
Pan band	96			544			473		

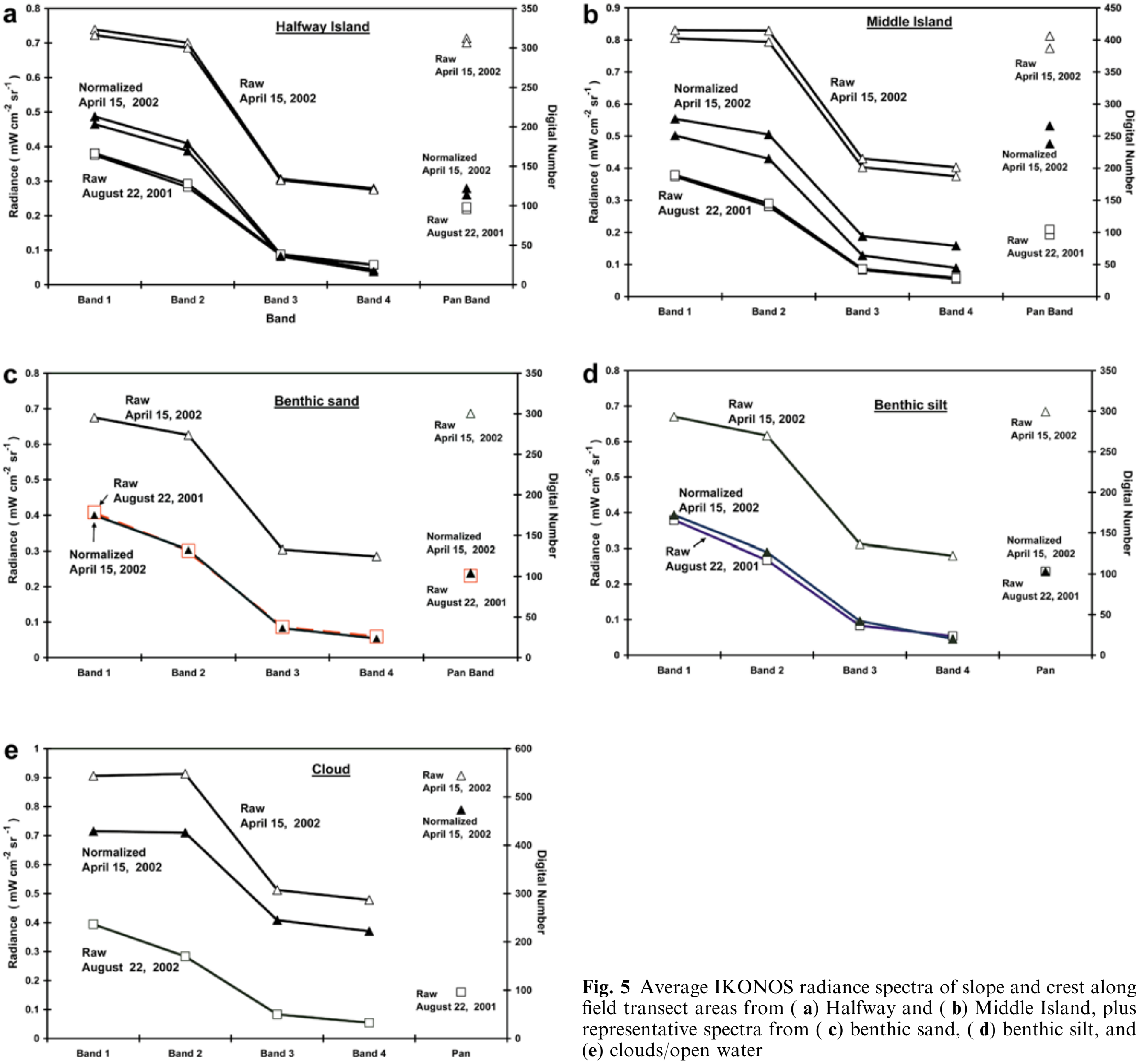

Fig. 5 Average IKONOS radiance spectra of slope and crest along field transect areas from (**a**) Halfway and (**b**) Middle Island, plus representative spectra from (**c**) benthic sand, (**d**) benthic silt, and (**e**) clouds/open water

band. This pattern is most obvious in the spectra from Halfway Island, where the normalized April 15 spectra are 30% brighter than the August spectra in band 1, and 44% brighter in band 2. After radiometric normalization, the April and August transect spectra from Halfway Island have essentially the same DN values in bands 3 and 4. Since clear water has nearly zero reflectance in band 4, these results indicate that the radiometric normalization performed well at Halfway Island.

The Middle Island spectra also indicated that the bleaching was detected in bands 1 and 2, though not as clearly as Halfway Island. Even after the radiometric normalization, the April spectra yield higher DN values than the August spectra in band 3, band 4, and the panchromatic band. We concluded that the radiometric normalization was only partially successful due to the variable thin cloud cover present in the April image.

Radiance spectra from the two other benthic cover types (white sand and silt) showed little change from August to April (Fig. 5). The submerged white sand has a similar spectral signature to the bleached coral and could be confused for bleached coral if only one image were available. The ability to distinguish bleached coral from submerged white sand is based on the change in coral spectrum between dates of imagery. In contrast, radiance spectra of clouds are brighter in all spectral bands (Fig. 5) and are readily distinguished from the bleached coral.

By combining the first three image difference bands (1, 2, 3 as red, green, and blue) to form a color composite and applying a contrast stretch the location of the bleached coral could be readily discerned based on their gold tone (Fig. 6). Benthic areas with little or no spectral change remain dark in the color composite. Because the brightening associated with the bleaching was only expressed in bands 1 and 2 of the IKONOS data, it was possible to distinguish this from the brightening associated with cloud cover in the April image (clouds are bright in all the IKONOS bands). A total of 0.2326 km^2 of bleached coral were detected surrounding Halfway Island and 0.0799 km^2 were detected at Middle Island. When applied to the full scene, it is possible to identify several additional areas of coral bleaching in nearshore waters in the eastern half of Great Keppel Island (Fig. 6). Some portions of the April image had too much cloud cover for unambiguous interpretation of the results. A total of 0.4295 km^2 of bleached coral was detected in waters surrounding Great Keppel Island.

Discussion

Change detection analysis

We have proposed a technique for detecting bleached coral areas through an examination of a pair of radiometrically normalized IKONOS imagery from areas known to have experienced extensive bleaching based on underwater transects. The technique requires the availability of an image acquired during a bleaching event and a second image acquired prior to the bleaching or following the recovery from the bleaching. The pseudo-invarient feature (PIF) relative radiometric normalization method we employed assumes that the light and dark pixel sets changed little between the image collection dates and that the factors responsible for producing radiometric differences in the PIFs exert the same influence in other part of the scenes. While it is acknowledged that these assumptions are not absolutely true in our case because of the cloud cover, they nevertheless generally enable the detection of interpretable spectral changes where benthic features can be observed in both dates of imagery (Andréfouët et al. 2001).

A wide range of factors act to shift benthic scene radiometry, including changes in the sensor, solar irradiance, viewing geometry, as well as atmospheric and water column differences. Ideally, addressing the radiometric differences between scenes consists in converting each image DN to reflectance units (Yamano and Tamura 2001) and then observing the differences. There are two primary methods for such a conversion: empirical line calibration and radiative transfer modeling. Implementation of the empirical line calibration requires the availability of reflectance spectra from the field. The radiative transfer model needs to be parameterized with extensive sets of field measurements (solar irradiance, aerosol optical thickness, and the inherent optical properties of the water column) acquired at the time of the satellite data. In our case, we didn't have any of these in situ measurements. We could have used data

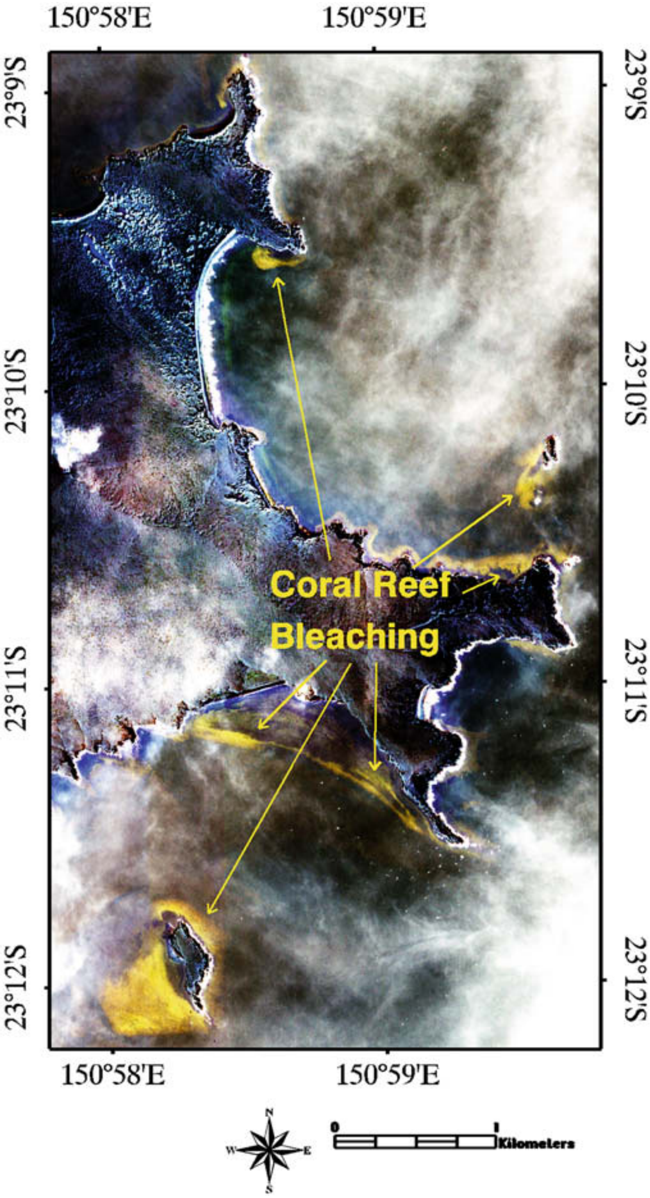

Fig. 6 Color composite image (R = Band 1, G = Band 2, B = Band 3) of the eastern portion of the Keppel Islands formed with radiometrically normalized IKONOS band difference data. An equalization stretch accentuates the spectral differences within the scene, highlighting bleached reef areas in bright gold color

for other sites, but without guarantee that they would be adequate. Therefore, we selected a relative radiometric normalization approach to remove most of the radiometric differences between the two scenes prior to the analysis of spectral changes. This also has the benefit of preserving the original data values in one of the images, reducing the introduction of errors inherent to any radiometric transformation.

The strategy of a relative radiometric normalization is to bundle the effects of all of the factors contributing to radiometric differences between a reference scene and a subject scene, assuming some areas are stable. Where changes were detected, we assumed that they were due to change in bottom reflectance. Indeed, the drawback of our approach compared to an analytical one is that we can't conduct a sensitivity analysis to assess the potential noise due to other factors, in the water (e.g. change in colored dissolved organic matter or chlorophyll concentration) or in the atmosphere (cloud thickness). However, the spatial patterns of changes were clear enough (Fig. 6), despite the variations in cloud optical thickness, to conclude positively that these changes are due to bottom changes and bleaching.

IKONOS sensitivity for bleaching detection

The results indicate that bleaching was detected as a brightening in the IKONOS bands 1 and 2, but not in bands 3, 4, or the panchromatic band. This constitutes a change spectral signature for bleached coral. The selective detection of the bleaching in bands 1 and 2 is likely the result of greater penetration of sunlight through the water column in these two spectral bands and the higher incoming solar irradiance in the blue and green end of the spectrum. The integration along the IKONOS spectral sensitivity curves of the diffuse attenuation coefficients provided by Smith and Baker (1981) for clear waters yield the values 0.034, 0.087, and 0.405 (in m^{-1}) in bands 1, 2, and 3, respectively. Thus, the four multispectral bands can be generally ranked based on the intensity of water absorption as Band 4 > > > Band 3 > > Band 2 > Band 1.

Methodological perspectives

The extensive coral cover (greater than 70%) and the high level of white bleaching (greater than 90% of coral cover) prevented developing a spectral change index related to the extent or severity of bleaching. While a change spectral index is feasible in theory, it can be anticipated that it would respond both to the severity of bleaching and the fractional cover of coral. This is the case for most other remotely sensed spectral indices. In our case study, the range of coral cover and bleaching values are too narrow and too high to define this index. The set of GBR sites processed by Andréfouët et al. (2002) would provide such gradients with contrasting patterns of coral cover and bleaching intensity, but no IKONOS images were available before or during the 1998 event on which analyses were based. Field observations and an examination of a bathymetric chart indicate that bleached coral was detected in waters as deep as 15 m.

It seems also possible to photo-interpret the presence of bleaching in black-and-white difference images produced from either bands 1 or 2. In our case, these images contained brightness differences induced by variations in the density of thin cloud cover in the April 15, 2002 IKONOS scene, which complicated automatic identification of the bleaching. For other case studies with optimal data, a mono-band processing could be a quick and effective solution. However, a better visual strategy is to make use of color composites of the band 1, 2, and 3 difference images. It was possible to clearly discern areas of bleached coral, which show up as a gold color in color composites made with differences images from bands 1, 2, and 3, displayed as red, green, and blue. In our case, this approach is particularly effective because clouds are bright in all the IKONOS bands, while bleached reef is brighter only in bands 1 and 2. Benthic surfaces (e.g. sand, silt, sea grass, algal beds) which experienced little change between the dates of imagery will tend to be dark in each band difference images. This band difference color composite of the entire IKONOS coverage area revealed extensive areas of bleached coral at other sites near our study area, such as the east end of Great Keppel Island, a deep platform to the east of Middle Island, the west side of Halfway Island, and along the eastern exposed shores of Halfway Island. Interestingly, these sites were not known for their high coral cover.

In the case of presence of clouds, it may be possible to devise a radiometric normalization that would compensate for variable thin cloud cover. The proportion of cloud and water contributing the signal measured in a pixel may be amenable to spectral mixture analysis techniques. Alternatively, variations in the DN values of pixels containing open water (near zero reflectance) may provide a basis for a radiometric adjustment to each of the spectral bands that would adaptively correct for the influence of variable thin cloud cover. If successful, this approach may make it possible to identify coral bleaching in imagery contaminated by variable thin cloud cover.

Implications for reef monitoring and management

There are several implications of this study for managers and scientists interested in monitoring bleaching. First, our method relies on the availability of a pre-bleaching image to serve as a reference. While it may be possible to identify bleached coral in a single image acquired at or near the peak in bleaching, it will always be more irrefutable to base the analysis on comparison to a recent reference image acquired before bleaching. This provides one more justification for building archives of satellite images in key environmentally significant areas, such as coral reefs. It may be possible to use historical color aerial photographs in lieu of pre-bleaching satellite imagery (Palandro et al. 2003), but this implies more calibration issues. Second, any project planning to use IKONOS or similar high spatial resolution satellite imagery (QUICKBIRD, EROS) for widespread mapping of coral bleaching should consider having a pre-established contract with their imagery provider, with associated acquisition constraints specified to ensure the best view of benthic features. This will allow the scheduling of new data acquisitions in specific areas with minimal delay. However, the spatial extent of new acquisitions may be limited by the cost of acquiring new imagery. The expedited IKONOS image acquisition made of the Keppel Islands cost nearly $10,000 dollars (US).

This study confirms that the qualitative (presence/absence of bleaching) detection of coral bleaching is possible using IKONOS data. However, with more than 70–90% live coral cover (of which 92–99% was white bleached coral), the example presented here is a "best-case" scenario in terms of the spatial extent of heavily bleached coral. For the Keppels, IKONOS imagery would have confirmed without any doubt an SST warning, but further case studies are required to generalize this positive result.

An unintended outcome of our study is the finding that it may be possible to make detailed maps of living coral while the coral is in a bleached state. Mapping accurately living coral cover on reefs using remotely sensed data traditionally relies on photo-interpretation of sub-meter scale color photography, and extensive knowledge of the site. Using bleached and non-bleached IKONOS band difference images we were able to clearly discern shallow water coral reef areas based on the brightening in bands 1 and 2. Thus heavy bleaching of corals may provide an unusually good situation for making detailed maps of coral reefs and devising a new sampling strategy. This is a useful capability and of considerable interest to reef managers.

In conclusion, while it was possible to detect coral bleaching using IKONOS imagery in our study area, this does not demonstrate that bleaching can be detected accurately for most of the reef configurations in the world. Reef managers interested in satellite remote sensing of coral bleaching should consider whether their areas of interest are suitable in terms of depth, coral cover, patchiness, and size of structures (Andréfouët et al. 2002). The fact that bleaching was detected in the Keppel Islands area using 4-m resolution data provides confirmation of some of the predictions made by Andréfouët et al. (2002). Managers may have also to consider alternative processing techniques (e.g. spectral unmixing) even if they have been tested so far only using laboratory experimental design and not using real airborne or satellite (Hedley et al. this issue). If found suitable, IKONOS change detection during bleaching events can provide the added bonus of accurately mapping areas which have (or had) high coral cover. We suggest that more sites should be tested during future bleaching events. Virtually all research reef sites of potential interest were covered by IKONOS images since 2000 (Andréfouët et al. in press). These images could serve as reference in the event that bleaching occurs. This would permit a fuller characterization of the capabilities of IKONOS and other high-spatial resolution data sources in detecting and quantifying coral bleaching, as a mapping tool for areas of high living coral cover, and to confirm SST-based coral bleaching warnings.

References

Andréfouët S, Berkelmans R, Odriozola L, Done T, Oliver J, Muller-Karger F (2002) Choosing the appropriate spatial resolution for monitoring coral bleaching events using remote sensing. Coral Reefs 21:147–154

Andréfouët S, Kramer P, Torres-Pulliza D, Joyce KE, Hochberg EJ, Garza-Perez R, Mumby PJ, Riegl B, Yamano H, White WH, Zubia M, Brock JC, Phinn SR, Naseer A, Hatcher BG, Muller-Karger FE (2003) Multi-site evaluation of IKONOS data for classification of tropical coral reef environments. Remote Sens Environ (in press)

Andréfouët S, Muller-Karger FE, Hochberg EJ, Hu C, Carder KL (2001) Change detection in shallow coral reef environments using Landsat 7 ETM+ data. Remote Sens Environ 78:150–162

Berkelmans R (2002) Time-integrated thermal bleaching thresholds of reefs and their variation on the Great Barrier Reef. Mar Ecol Prog Ser 229:73–82

Berkelmans R, De'ath G, Kininmonth S, Skirving W (2004) A comparison of the 1998 and 2002 bleaching events on the Great Barrier Reef: spatial correlation, patterns and predictions. Coral Reefs (this issue)

Berkelmans R, Oliver JK (1999) Large scale bleaching of corals on the Great Barrier Reef. Coral Reefs 18:55–60

Capolsini P, Andréfouët S, Rion C, Payri C (2004) A comparison of Landsat ETM+, SPOT HRV, Icons, ASTER and airborne MASTER data for coral reef habitat mapping in South Pacific islands. Can J Remote Sens (in press)

Christi CA, Bass DK, Neale, SJ, Osborne K, Oxley WG (1996) Surveys of sessile benthic communities using the video transect technique. Standard Operational Procedure No. 2, Australian Institute of Marine Science, Townsville

Clark CD, Mumby PJ, Chisholm JRM, Jaubert J, Andréfouët S (2000) Spectral discrimination of coral mortality states following a severe bleaching event. Int J Remote Sens 21:2321–2327

Diaz-Pulido G, McCook LJ (2002) The fate of bleached corals: patterns and dynamics of algal recruitment. Mar Ecol Progr Ser 232:115–128

Goreau TJ, Hayes RL (1994) Coral bleaching and ocean 'Hot Spots'. Ambio 3:176–180

Hedley JD, Mumby PJ, Joyce KE, Phinn SR (2004) Spectral unmixing of coral reef benthos under ideal conditions. Coral Reefs (this issue)

Hoegh-Guldberg O (1999) Climate change, coral bleaching and the future of the world's coral reefs. Mar Freshwater Res 50:217–224

Holden H, LeDrew E (1998) Spectral discrimination of healthy and non-healthy corals based on cluster analysis, principal components analysis, and derivative spectroscopy. Remote Sens Environ 65:217–224

Liu G, Skirving W, Strong A (2003) Remote sensing of sea surface temperatures during the 2002 Great Barrier Reef coral bleaching event. EOS (in press)

Mumby PJ, Edwards AJ (2002) Mapping marine environments with IKONOS imagery: enhanced spatial resolution can deliver greater thematic accuracy. Remote Sens Environ 82:248–257

Palandro D, Andréfouët S, Dustan P, Muller-Karger FE (2003) Change detection in coral reef communities using the IKONOS sensor and historic aerial photographs. Int J Remote Sens 24:873–878

Podestá GP, Glynn PW (1997) Sea surface temperature variability in Panama and Galapagos: extreme temperatures causing coral bleaching. J Geophys Res 102:15749–15759

Schott JR, Salvaggio C, Volchok WJ (1988) Radiometric scene normalization using pseuedo-invariant features. Remote Sens Environ 26:1–16

Smith RC, Baker KS (1981) Optical properties of the clearest natural waters (200–800 nm). Appl Opt 20:177–184

Wellington GM, Glynn PW, Strong AE, Navarrete SA, Wieters E, Hubbard D (2001) Crisis on coral reefs linked to climate change. EOS 82:1–5

Yamano H, Tamura M (2001) Use of Landsat TM data and radiative transfer models for monitoring coral reef bleaching. Proc the IGARSS 2001, Sydney, Australia (CDROM)